J|A|C|S
ARTICLES
Published on Web 10/31/2002

Metal Ion-Catalyzed Diels−Alder and Hydride Transfer Reactions. Catalysis of Metal Ions in the Electron-Transfer Step

Shunichi Fukuzumi,* Kei Ohkubo, and Toshihiko Okamoto

Contribution from the Department of Material and Life Science, Graduate School of Engineering, Osaka University and CREST, Japan Science and Technology Corporation (JST), Suita, Osaka 565-0871, Japan

Received April 4, 2002

Abstract: Rates of Diels−Alder cycloaddition of anthracenes with *p*-benzoquinone and its derivatives as well as rates of hydride-transfer reactions from 10-methyl-9,10-dihydroacridine to the same series of *p*-benzoquinones are accelerated significantly in the presence of metal ions in acetonitrile. An extensive comparison of the catalytic effects of metal ions in electron transfer from one-electron reductants (cobalt tetraphenylporphyrin and decamethylferrocene) to *p*-benzoquinones with those in the Diels−Alder reactions of the quinones as well as the hydride-transfer reactions has revealed that the catalysis of metal ions in each case is ascribed to the 1:1 and 1:2 complexes formed between the corresponding semiquinone radical anions and metal ions. The transient absorption and ESR spectra of the semiquinone radical anion−metal ion complexes are detected directly in the electron-transfer reduction of *p*-benzoquinone derivatives in the presence of metal ions. The catalytic reactivities of a variety of metal ions in each reaction are well correlated with the energy splitting values of π_g levels because of the complex formation between $O_2^{\bullet-}$ and M^{n+}, which are derived from the g_{zz} values of the ESR spectra of the $O_2^{\bullet-}-M^{n+}$ complex.

Introduction

Diels−Alder reactions are the most widely studied because of their great importance in the synthetic and theoretical fields, and they are generally believed to proceed via a thermally allowed concerted process.[1] However, there have recently been increasing interest in the important role of electron-transfer processes as the activation step for some Diels−Alder reactions of electron-rich dienes with high-lying HOMO and electron-deficient dienophiles with low-lying LUMO.[2−4] The photochemical cycloadditions via photosensitized electron-transfer and charge-transfer irradiation of the electron donor−acceptor complexes formed between dienes and dienophiles have also been well documented.[5−8] However, the possible contribution of electron transfer in thermal Diels−Alder reactions has so far been limited to those with powerful dienophiles being strong electron acceptors.[2−4] On the other hand, it is well-known that not only the rates of Diels−Alder reactions but also the regioselectivities and stereoselectivities are profoundly influenced by Lewis acid catalysts.[9−12] A variety of metal ions acting

* To whom correspondence should be addressed. E-mail: fukuzumi@ap.chem.eng.osaka-u.ac.jp.

(1) (a) Houk, K. N.; Evanseck, J. D. *Angew. Chem., Int. Ed. Engl.* **1992**, *31*, 682. (b) Houk, K. N.; Gonzalez, J.; Li, Y. *Acc. Chem. Res.* **1995**, *28*, 81. (c) Dewar, M. J. S.; Jie, C. *Acc. Chem. Res.* **1992**, *25*, 537. (d) Horn, B. A.; Herek, J. L.; Zewail, A. H. *J. Am. Chem. Soc.* **1996**, *118*, 8755. (e) Sustmann, R.; Tappanchai, S.; Bandmann, H. *J. Am. Chem. Soc.* **1996**, *118*, 12555. (f) Sauer, J.; Sustmann, R. *Angew. Chem., Int. Ed. Engl.* **1980**, *19*, 779.

(2) (a) Fukuzumi, S.; Kochi, J. K. *Tetrahedron* **1982**, *38*, 1035. (b) Sustmann, R. Korth, H.-G.; Nüchter, U.; Siangouri-Feulner, I.; Sicking, W. *Chem. Ber.* **1991**, *124*, 2811. (c) Fukuzumi, S.; Okamoto, T. *J. Am. Chem. Soc.* **1993**, *115*, 11600. (d) Rese, M.; Lucking, K.; Sustmann, R. *Liebigs Ann.* **1995**, 1139. (e) Sustmann, R.; Lücking, K.; Kopp, G.; Rese, M. *Angew. Chem., Int. Ed. Engl.* **1989**, *28*, 1713. (f) Lucking, K.; Rese, M.; Sustmann, R. *Liebigs Ann.* **1995**, 1129. (g) Wise, K. E.; Wheeler, R. A. *J. Phys. Chem. A* **1999**, *103*, 8279.

(3) (a) Yamago, S.; Ejiri, S.; Nakamura, M.; Nakamura, E. *J. Am. Chem. Soc.* **1993**, *115*, 5344. (b) Boger, D. L.; Brotherton, C. E. In *Advances in Cycloaddition*; D. P. Curran, Ed.; JAI Press: Greenwich, CT, 1990; Vol. 2, p 147. (c) Schmittel, M.; Wöhrle, C.; Bohn, I. *Chem.—Eur. J.* **1996**, *2*, 1031.

(4) (a) Kim, J. H.; Lindeman, S. V.; Kochi, J. K. *J. Am. Chem. Soc.* **2001**, *123*, 4951. (b) Kim, J. H.; Hubig, S. M.; Lindeman, S. V.; Kochi, J. K. *J. Am. Chem. Soc.* **2001**, *123*, 87.

(5) (a) Ledwith, A. *Acc. Chem. Res.* **1972**, *5*, 133. (b) Mattes, S. L.; Farid, S. *Acc. Chem. Res.* **1982**, *15*, 80. (c) Mattay, J.; Trampe, G.; Runsink, J. *Chem. Ber.* **1988**, *121*, 1991. (d) Lewis, F. D. *Photoinduced Electron Transfer*; Fox, M. A., Chanon, M., Eds.; Elsevier: Amsterdam, 1988; Part C, p 1. (e) Gotoh, T.; Padias, A. B.; Hall, H. K., Jr. *J. Am. Chem. Soc.* **1991**, *113*, 1308. (f) Bauld, N. L. *Advances in Electron-Transfer Chemistry*; Mariano, P. S., Ed.: JAI Press: Greenwich, CT, 1992; Vol. 2, p 1.

(6) (a) Takahashi, Y.; Kochi, J. K. *Chem. Ber.* **1988**, *121*, 253. (b) Kim, E.; Christl, M.; Kochi, J. K. *Chem. Ber.* **1990**, *123*, 1209. (c) Sun, D.; Hubig, M.; Kochi, J. K. *J. Photochem. Photobiol., A* **1999**, *122*, 87.

(7) (a) Mikami, K.; Matsumoto, S.; Okubo, Y.; Fujitsuka, M.; Ito, O.; Suenobu, T.; Fukuzumi, S. *J. Am. Chem. Soc.* **2000**, *122*, 2236. (b) Vassilikogiannakis, G.; Orfanopoulos, M. *Tetrahedron Lett.* **1997**, *38*, 4323. (c) Mikami, K.; Matsumoto, S.; Tonoi, T.; Okubo, Y.; Suenobu, T.; Fukuzumi, S. *Tetrahedron Lett.* **1998**, *39*, 3733.

(8) Müller, F.; Mattay, J. *Chem. Rev.* **1993**, *93*, 99.

(9) (a) Paquette, L. A. In *Asymmetric Synthesis*; Morison, J. D., Ed.; Academic Press: New York, 1984; Vol. 3, pp 456−478. (b) Oppolzer, W. *Angew. Chem., Int. Ed. Engl.* **1984**, *23*, 876. (c) Sauer, J.; Sustmann, R. *Angew. Chem., Int. Ed. Engl.* **1980**, *19*, 779. (d) Bonnesen, P. V.; Puckett, C. L.; Honeychuck, R. V.; Hersh, W. H. *J. Am. Chem. Soc.* **1989**, *111*, 6070.

(10) (a) Otto, S.; Engberts, J. B. F. N. *J. Am. Chem. Soc.* **1999**, *121*, 6798. (b) Otto, S.; Boccaletti, G.; Engberts, J. B. F. N. *J. Am. Chem. Soc.* **1998**, *120*, 4238. (c) Otto, S.; Bertoncin, F.; Engberts, J. B. F. N. *J. Am. Chem. Soc.* **1996**, *118*, 7702. (d) Pindur, U.; Lutz, G.; Otto, C. *Chem. Rev.* **1993**, *93*, 741. (e) Fringuelli, F.; Piermatti, O.; Pizzo, F.; Vaccaro, L. *Eur. J. Org. Chem.* **2001**, 439.

as Lewis acids are also known to accelerate electron-transfer reactions of carbonyl compounds significantly.[13−15] Metal ions can also accelerate hydride-transfer reactions from NADH (dihydronicotinamide adenine dinucleotide) model compounds to carbonyl compounds via metal ion-catalyzed electron transfer as the rate-determining step.[16,17] However, it has yet to be clarified how the Lewis acid catalysis in electron-transfer reactions of carbonyl compounds such as *p*-benzoquinones is correlated with the catalysis in Diels−Alder reactions and hydride-transfer reactions of the same *p*-benzoquinones acting as dienophiles and hydride acceptors, respectively.

We report, herein, that a variety of metal ions act as effective catalysts to accelerate Diels−Alder reactions of anthracenes with *p*-benzoquinone derivatives, which have been regarded as inert or weak dienophiles.[18] Scandium triflate ($Sc(OTf)_3$) is shown to be by far the most reactive as compared to other metal ions.[19] An extensive comparison of the catalysis of a series of metal ions has been performed for the first time among the electron-transfer reactions, the Diels−Alder reactions, and the hydride-transfer reactions of *p*-benzoquinones acting as electron acceptors, dienophiles, and hydride acceptors, respectively. The direct spectroscopic detection of complexes formed between the corresponding semiquinone radical anions and metal ions, combined with the detailed kinetic analysis of the catalytic effects of metal ions, provides a confirmative basis to delineate the common catalytic mechanism of metal ions in each reaction.

Experimental Section

Materials. Anthracene and its derivatives (9,10-dimethylanthracene, 9-methylanthracene, 9-ethylanthracene, 9-benzylanthracene, and 9-bromoanthracene) were obtained commercially. *p*-Benzoquinone and its derivatives (2,5-dimethyl-*p*-benzoquinone, 2,5-dichloro-*p*-benzoquinone, *p*-fluoranil, and *p*-chloranil) were also obtained commercially and purified by the standard methods.[20] Decamethylferrocene (Sigma) and 1,1′-dimethylferrocene (Tokyo Kasei Organic Chemicals) were commercially available. Cobalt(II) tetraphenylporphyrin (CoTPP) was prepared as given in the literature.[21] The dimeric 1-benzyl-1,4-dihydronicotinamide [$(BNA)_2$] was prepared according to the literature.[22] 9,10-Dihydro-10-methylacridine ($AcrH_2$) was prepared from 10-methylacridinium iodide ($AcrH^+I^-$) by reduction with $NaBH_4$ in methanol and purified by recrystallization from ethanol.[23] Scandium triflate [$Sc(OTf)_3$] was purchased from Pacific Metals Co., Ltd. (Taiheiyo Kinzoku). Lanthanum triflate [$La(OTf)_3$] was obtained from Aldrich in hexahydrate form. Yttrium triflate [$Y(OTf)_3$], europium triflate [$Eu(OTf)_3$], ytterbium triflate [$Yb(OTf)_3$], and lutetium triflate [$Lu(OTf)_3$] were prepared as follows.[24] A deionized aqueous solution was mixed (1:1 v/v) with trifluoromethanesulfonic acid (>99.5%, 10.6 mL) obtained from Central Glass, Co., Ltd., Japan. The trifluoromethanesulfonic acid solution was slowly added to a flask which contained the corresponding metal oxide (>99.9%, 30 mmol). The mixture was refluxed at 100 °C for 3 days. After centrifugation of the reaction mixture, the solution containing metal triflate was separated and water was removed by vacuum evaporation. Yttrium oxide, europium oxide, and ytterbium triflate were purchased from Shin Etsu Chemical, Co., Ltd., Japan. Lutetium oxide was obtained from Nichia Corporation, Japan. Metal triflates were dried under vacuum evacuation at 403 K for 40 h prior to use. Magnesium perchlorate [$Mg(ClO_4)_2$] was obtained from Wako Pure Chemical Ind. Ltd., Japan. Calcium perchlorate [$Ca(ClO_4)_2$] was obtained from Nacalai Tesque, Japan. Acetonitrile (MeCN) used as a solvent was purified and dried by the standard procedure.[20]

Reaction Procedure and Analysis. Typically, an [$^2H_3$]acetonitrile (CD_3CN) solution (0.7 cm^3) containing an anthracene derivative (1.0×10^{-2} M) and *p*-benzoquinone derivatives (2.0×10^{-2} M) in the presence (1.0 M) and absence of $Mg(ClO_4)_2$ in an NMR tube sealed with a rubber septum was deaerated by bubbling with argon gas through a stainless steel needle for 5 min and was mixed. Several hours later, the reaction solution was analyzed by ^1H NMR spectroscopy. The ^1H NMR measurements were performed using a Japan Electron Optics JNM-GSX-400 (400 MHz) NMR spectrometer at 300 K. ^1H NMR (CD_3CN in the presence of 1.0 M $Mg(ClO_4)_2$). **1a**: δ 1.98 (s, 6H), 2.85 (s, 2H), 6.12 (s, 2H), 7.22−7.31 (m, 6H), 7.45−7.49 (m, 2H). **1b**: δ 1.91 (s, 3H), 2.01 (s, 3H), 3.29 (s, 1H), 6.50 (s, 1H), 7.24−7.39 (m, 6H), 7.50−7.57 (m, 2H). **1c**: δ 0.88 (s, 3H), 1.59 (s, 3H), 1.85 (s, 3H), 1.90 (s, 3H), 2.39 (s, 1H), 5.87 (s, 1H), 7.15−7.32 (m, 6H), 7.42−7.50 (m, 2H). **1d**: δ 1.98 (s, 3H), 2.77 (d, 1H, J = 8.8 Hz), 3.24 (dd, 1H, J = 2.9, 8.8 Hz), 4.73 (d, 1H, J = 2.9 Hz), 6.17, 6.26 (ABq, 2H, J = 10.26 Hz), 7.17−7.27 (m, 6H), 7.43−7.50 (m, 2H). **1e**: δ 3.21 (s, 2H), 4.86 (s, 2H), 6.40 (s, 2H), 7.04−7.24 (m, 6H), 7.43−7.50 (m, 2H).

Spectral Measurements. Transient absorption spectra of 1:1 and 1:2 complexes of semiquinone radical anions ($X-Q^{\bullet-}$) with Mg^{2+} were measured by using a Union RA-103 stopped-flow spectrophotometer. The transient absorption spectra of the Mg^{2+} complexes were obtained by plotting the initial absorbances in the kinetic curves against the wavelengths in the electron-transfer reduction of *p*-benzoquinone derivatives (2.4×10^{-3} M) by [$Fe(Me_5C_5)_2$] or [$Fe(MeC_5H_4)_2$] (2.4×10^{-4} M) in the presence of various concentrations of Mg^{2+} in deaerated MeCN at 298 K.

Kinetic Measurements. Kinetic measurements were performed on a Hewlett-Packard 8453 photodiode array spectrophotometer. Rates of Diels−Alder reactions of anthracene derivatives (6.2×10^{-4}−1.3×10^{-3} M) with *p*-benzoquinone derivatives (1.8×10^{-2}−3.8×10^{-1} M) in the presence and absence of metal ion were monitored by measuring

(11) (a) Doyle, M. P.; Phillips, I. M.; Hu, W. *J. Am. Chem. Soc.* **2001**, *123*, 5366. (b) Evans, D. A.; Miller, S. J.; Lectka, T.; von Matt, P. *J. Am. Chem. Soc.* **1999**, *121*, 7559. (c) Roush, W. R.; Barda, D. A. *J. Am. Chem. Soc.* **1997**, *119*, 7402.
(12) (a) Kumar, A. *Chem. Rev.* **2001**, *101*, 1. (b) Kagan, H. B.; Riant, O. *Chem. Rev.* **1992**, *92*, 1007. (c) Molander, G. A. *Chem. Rev.* **1992**, *92*, 29.
(13) (a) Fukuzumi, S.; Itoh, S. In *Advances in Photochemistry*; Neckers, D. C., Volman, D. H., von Bünau, G., Eds.; Wiley: New York, 1998; Vol. 25, pp 107−172. (b) Fukuzumi, S.; Satoh, N.; Okamoto, T.; Yasui, K.; Suenobu, T.; Seko, Y.; Fujitsuka, M.; Ito, O. *J. Am. Chem. Soc.* **2001**, *123*, 7756. (c) Fukuzumi, S.; Mori, H.; Imahori, H.; Suenobu, T.; Araki, Y.; Ito, O.; Kadish, K. M. *J. Am. Chem. Soc.* **2001**, *123*, 12458.
(14) (a) Fukuzumi, S. In *Electron Transfer in Chemistry*; Balzani, V., Ed.; Wiley-VCH: Weinheim, Germany, 2001; Vol. 4, pp 3−67. (b) Fukuzumi, S. *Bull. Chem. Soc. Jpn.* **1997**, *70*, 1.
(15) Fukuzumi, S.; Ohkubo, K. *Chem.—Eur. J.* **2000**, *6*, 4532.
(16) (a) Fukuzumi, S.; Koumitsu, S.; Hironaka, K.; Tanaka, T. *J. Am. Chem. Soc.* **1987**, *109*, 305. (b) Fukuzumi, S.; Nishizawa, N.; Tanaka, T. *J. Chem. Soc., Perkin Trans. 2* **1985**, 371−378.
(17) Fukuzumi, S.; Fujii, Y.; Suenobu, T. *J. Am. Chem. Soc.* **2001**, *123*, 10191.
(18) (a) Kanematsu, K.; Morita, S.; Fukushima, S.; Osawa, E. *J. Am. Chem. Soc.* **1981**, *103*, 5211. (b) Finley, K. T. *The Chemistry of the Quinoid Compounds*; Patai, S., Ed.; Wiley-Interscience: New York, 1974; Part 2, p 877.
(19) Lithium perchlorate in diethyl ether has been reported to accelerate Diels−Alder reactions. The role of Li^+ has been discussed extensively. (a) Grieco, P. A.; Nunes, J. J.; Gaul, M. D. *J. Am. Chem. Soc.* **1990**, *112*, 4595. (b) Waldmann, H. *Angew. Chem., Int. Ed. Engl.* **1991**, *30*, 1306. (c) Smith, D. A.; Houk, K. N. *Tetrahedron Lett.* **1991**, *32*, 1549. (d) Forman, M. A.; Dailey, W. P. *J. Am. Chem. Soc.* **1991**, *113*, 2761. (e) Desimoni, G.; Faita, G.; Righetti, P. P.; Tacconi, G. *Tetrahedron* **1991**, *47*, 8399. (f) Pagni, R. M.; Kabalka, G. W.; Bains, S.; Plesco, M.; Wilson, J.; Bartmess, J. *J. Org. Chem.* **1993**, *58*, 3130. (g) Jiao, H.; Schleyer, P. v. R. *J. Am. Chem. Soc.* **1995**, *117*, 11529. (h) Kumar, A. *J. Org. Chem.* **1994**, *59*, 4612. (i) Kumar, A.; Pawar, S. S. *J. Org. Chem.* **2001**, *66*, 7646.
(20) Perrin, D. D.; Armarego, W. L. F. *Purification of Laboratory Chemicals*; Butterworth-Heinemann: Oxford, U.K.,1988.
(21) Adler, A. D.; Longo, F. R.; Váradi, V. *Inorg. Synth.* **1976**, *16*, 213.
(22) (a) Wallenfels, K.; Gellerich, M. *Chem. Ber.* **1959**, *92*, 1406. (b) Patz, M.; Kuwahara, Y.; Suenobu, T.; Fukuzumi, S. *Chem. Lett.* **1997**, 567.
(23) Fukuzumi, S.; Tokuda, Y.; Kitano, T.; Okamoto, T.; Otera, J. *J. Am. Chem. Soc.* **1993**, *115*, 8960.
(24) (a) Forsberg, J. H.; Spaziano, V. T.; Balasubramanian, T. M.; Liu, G. K.; Kinsley, S. A.; Duckworth, C. A.; Poteruca, J. J.; Brown, P. S.; Miller, J. L. *J. Org. Chem.* **1987**, *52*, 1017. (b) Kobayashi, S.; Hachiya, I. *J. Org. Chem.* **1994**, *59*, 3590.

the disappearance of absorbance due to 9,10-dimethylanthracene at $\lambda_{max} = 398$ nm ($\epsilon = 7.5 \times 10^3$ M^{-1} cm^{-1}), 9-methylanthracene at $\lambda_{max} = 386$ nm ($\epsilon = 6.6 \times 10^3$ M^{-1} cm^{-1}), and anthracene at $\lambda_{max} = 376$ nm ($\epsilon = 5.4 \times 10^3$ M^{-1} cm^{-1}) in MeCN. Measurements of rates of electron-transfer reactions from CoTPP to *p*-benzoquinone derivatives in the presence of a metal ion were performed using a Union RA-103 stopped-flow spectrophotometer. Rates of electron-transfer reactions from CoTPP (9.3×10^{-6} M) to *p*-benzoquinone derivatives (1.0×10^{-4}–1.2×10^{-3} M) were monitored by the rise and decay of the absorption band at 434 and 412 nm because of $CoTPP^+$ and CoTPP, respectively. Rates of hydride transfer from $AcrH_2$ (3.5×10^{-3}–1.0×10^{-2} M) to *p*-benzoquinone derivatives (1.0×10^{-4} M) were determined from the appearance of the absorbance due to 10-methylacridinium ion ($AcrH^+$: $\lambda_{max} = 358$ nm, $\epsilon_{max} = 1.80 \times 10^4$ M^{-1} cm^{-1}). All the kinetic measurements were carried out under pseudo-first-order conditions, where the concentrations of *p*-benzoquinone derivatives were maintained at >10-fold excess of the concentrations of anthracenes, CoTPP, or $AcrH_2$ at 298 or 333 K. Pseudo-first-order rate constants were determined by least-squares curve fits using a personal computer.

Cyclic Voltammetry. Cyclic voltammetry measurements were performed at 298 K on a BAS 100-W electrochemical analyzer in deaerated MeCN containing 0.1 M Bu_4NClO_4 (TBAP) as the supporting electrolyte. A conventional three-electrode cell was used with a platinum working electrode (surface area of 0.3 mm^2) and a platinum wire as the counter electrode. The Pt working electrode (BAS) was routinely polished with a BAS polishing alumina suspension and rinsed with acetone before use. The measured potentials were recorded with respect to the $Ag/AgNO_3$ (0.01 M) reference electrode. All potentials (vs Ag/Ag^+) were converted to values versus SCE by adding 0.29 V.[25] All electrochemical measurements were carried out under an atmospheric pressure of argon.

ESR Measurements. The *p*-fluoranil radical anion was prepared from *p*-fluoranil by reduction with $(BNA)_2$ in deaerated MeCN at 298 K. Typically, $(BNA)_2$ (2.0 mg) was put inside an Ar-purged ESR cell with the diameter of 0.8 mm and set in the ESR cavity at 243 K. *p*-Fluoranil was dissolved in MeCN (1.8 mg; 2.0×10^{-3} M in 1 mL) and purged with argon for 10 min. $Sc(OTf)_3$ (1.0 mg; 2.0×10^{-3} M in 1 mL) was also dissolved in deaerated acetonitrile. The *p*-fluoranil solution (200 μL) and $Sc(OTf)_3$ solution (200 μL) were introduced into the ESR cell and mixed by bubbling with Ar gas through a syringe with a long needle at 243 K. The ESR spectra of the radical anions of 2,5-dichloro-*p*-benzoquinone and 2,5-dimethyl-*p*-benzoquinone were measured at 213 K under the irradiation of light with a high-pressure mercury lamp (USH-1005D) focusing at the sample cell in the ESR cavity. The ESR spectra were measured with a JEOL X-band spectrometer (JES-RE1XE). The ESR spectra were recorded under nonsaturating microwave power conditions. The magnitude of modulation was chosen to optimize the resolution and the signal-to-noise (*S*/*N*) ratio of the observed spectra. The *g* values were calibrated with an Mn^{2+} marker. Computer simulation of the ESR spectra was carried out by using Calleo ESR version 1.2 (Calleo Scientific Publisher) on a Macintosh personal computer.

Results and Discussion

Catalysis of Metal Ions on Electron Transfer and Diels–Alder Reactions. Although the reaction of 9,10-dimethylanthracene (DMA 1.5×10^{-2} M) and *p*-benzoquinone (Q 2.5×10^{-2} M) is sluggish in MeCN at 298 K, the addition of $Sc(OTf)_3$ results in the efficient [4+2] cycloaddition to yield the adduct selectively (eq 1).

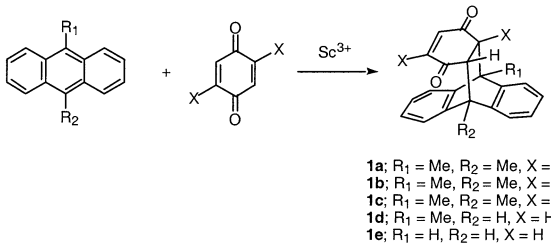

(1)

1a; R_1 = Me, R_2 = Me, X = H
1b; R_1 = Me, R_2 = Me, X = Cl
1c; R_1 = Me, R_2 = Me, X = Me
1d; R_1 = Me, R_2 = H, X = H
1e; R_1 = H, R_2 = H, X = H

The [4+2] cycloaddition of anthracene and 9-methylanthracene with other *p*-benzoquinone derivatives (X–Q; X = 2,5-Cl_2 and 2,5-Me_2) also occurs efficiently in the presence of Sc^{3+} to yield the corresponding adducts quantitatively (see Experimental Section).

The rates of reactions of Sc^{3+}-catalyzed Diels–Alder reactions of DMA with Q were determined by monitoring the disappearance of absorbance due to DMA ($\lambda_{max} = 398$ nm, $\epsilon_{max} = 7.5 \times 10^3$ M^{-1} cm^{-1}). The rates obeyed pseudo-first-order kinetics in the presence of large excesses of Q and Sc^{3+} relative to the concentration of DMA. The pseudo-first-order rate constant increases proportionally with Q concentration (see Supporting Information, S1). Thus, the rate exhibits the second-order kinetics showing a first-order dependence on each reactant concentration.

The dependence of the observed second-order rate constant (k_{obs}) on [Sc^{3+}] was examined for the Sc^{3+}-catalyzed Diels–Alder reaction of DMA with Q at various concentrations of Sc^{3+}. The k_{obs} value increases with an increase in [Sc^{3+}] to exhibit a first-order dependence on [Sc^{3+}] at low concentrations, changing to a second-order dependence at high concentrations, as shown in Figure 1a.

Such a mixture of first-order and second-order dependence on [Sc^{3+}] is also observed in the electron transfer from CoTPP (TPP^{2-} = tetraphenylporphyrin dianion) to Q. No electron transfer from CoTPP to Q has occurred in MeCN at 298 K. In the presence of $Sc(OTf)_3$, however, an efficient electron transfer from CoTPP to Q occurs to yield $CoTPP^+$ (eq 2).

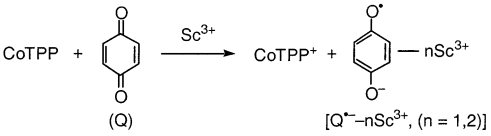

(2)

The electron transfer rates also obeyed second-order kinetics, showing a first order dependence on each reactant concentration. The dependence of the observed electron-transfer rate constant (k_{et}) on [Sc^{3+}] was also examined for the electron transfer from CoTPP to Q at various concentrations of Sc^{3+}. The results are shown in Figure 1b, where the k_{et} value increases linearly with [Sc^{3+}] to show a first-order dependence on [Sc^{3+}] at low concentrations, changing to a second-order dependence at high concentrations, as the case of the Sc^{3+}-catalyzed Diels–Alder reaction of DMA with Q in Figure 1a.

Other metal ions such as Mg^{2+} also exhibit a mixture of first-order and second-order dependence on the metal ion concentration, as shown in Figure 2a for the Mg^{2+}-catalyzed Diels–Alder reaction of DMA with Q as well as electron transfer from CoTPP to Q (Figure 2b).

There is no interaction between Q and Sc^{3+} or Mg^{2+}, as indicated by the lack of UV–vis spectral change of Q in the

(25) Since the metal ion is bound to the reaction product (eq 2), the reaction is called "M^{n+}-promoted" electron transfer. In the case of the Diels–Alder reactions (eq 1), the metal ion acts as a real catalyst.

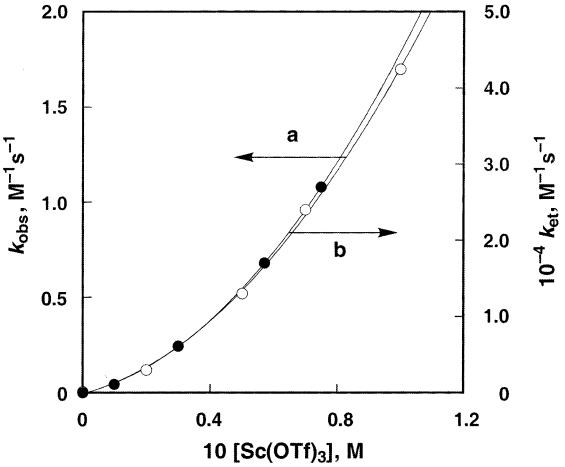

Figure 1. (a) Dependence of k_{obs} on [$Sc(OTf)_3$] for the Diels−Alder reaction of 9,10-dimethylanthracene (2.5×10^{-4} M) with *p*-benzoquinone (2.5×10^{-2} M) and (b) electron transfer from CoTPP (8.0×10^{-6} M) to *p*-benzoquinone (2.6×10^{-4} M) in the presence of $Sc(OTf)_3$ in deaerated MeCN at 298 K.

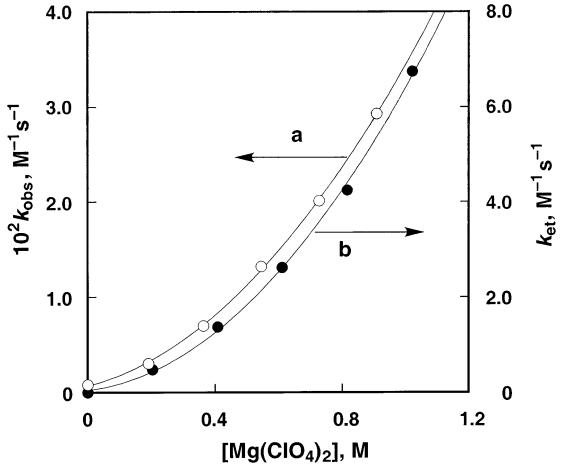

Figure 2. Dependence of k_{obs} on [$Mg(ClO_4)_2$] for the (a) Diels−Alder reaction of 9,10-dimethylanthracene (1.3×10^{-3} M) with *p*-benzoquinone (3.6×10^{-1} M) and (b) electron transfer from CoTPP (1.0×10^{-5} M) to *p*-benzoquinone (3.7×10^{-3} M) in the presence of $Mg(ClO_4)_2$ in deaerated MeCN at 298 K.

presence of the metal ion. The ^{13}C NMR signals of Q exhibited only small upfield shifts in the presence of large concentrations of $Mg(ClO_4)_2$ in CD_3CN. The observed chemical shifts ($\Delta\delta$) of the C═O and the C═C carbons of Q referenced to those in the absence of Mg^{2+} (see Supporting Information, S2). The $\Delta\delta$ value increases linearly with an increase in [$Mg(ClO_4)_2$], indicating that Q forms only a very weak 1:1 complex with Mg^{2+} in MeCN. Such a 1:1 complex with Mg^{2+}, however, cannot account for the contribution of the second-order dependence of the rate constants on [Mg^{2+}] in the electron transfer and Diels−Alder reactions, as shown in Figures 2. In such a case, the acceleration of electron transfer from CoTPP to Q is ascribed to the complexation of the metal ion (M^{n+}) with $Q^{\bullet-}$. Since there are two carbonyl oxygens which can interact with M^{n+}, $Q^{\bullet-}$ may form not only a 1:1 complex ($n = 1$ in eq 2) but also a 1:2 complex ($n = 2$ in eq 2) with M^{n+}. The complex formation of $Q^{\bullet-}$ and M^{n+} should result in the positive shift of the one-electron reduction potential of Q (E_{red}), and the Nernst equation is given by eq 3,

$$E_{red} = E^{\circ}_{red} + (2.3RT/F)\log\{K_1[M^{n+}](1 + K_2[M^{n+}])\} \quad (3)$$

where E°_{red} is the one-electron reduction potential of Q in the absence of M^{n+}; K_1 and K_2 are the formation constants for the 1:1 and 1:2 complexes between $Q^{\bullet-}$ and M^{n+}, respectively.[27] Since M^{n+} has no effect on the oxidation potential of CoTPP, the free energy change of electron transfer from CoTPP to Q in the presence of M^{n+} (ΔG_{et}) can be expressed by eq 4,

$$\Delta G_{et} = \Delta G^{\circ}_{et} - (2.3RT)\log(K_1[M^{n+}] + K_1K_2[M^{n+}]^2) \quad (4)$$

where ΔG°_{et} is the free energy change of electron transfer in the absence of M^{n+}. The ΔG°_{et} value is obtained from the one-electron oxidation potential of CoTPP (E°_{ox} vs SCE = 0.35 V)[28] and the one-electron reduction potential of Q (E°_{red} vs SCE = −0.50 V) by using eq 5.

$$\Delta G^{\circ}_{et} = F(E^{\circ}_{ox} - E^{\circ}_{red}) \quad (5)$$

In the presence of M^{n+}, E°_{red} in eq 5 is replaced by eq 3. Thus, electron transfer from CoTPP to Q becomes more favorable energetically with an increase in the concentration of M^{n+}. If such a change in the energetics is directly reflected in the transition state of electron transfer, the dependence of the observed rate constant of electron transfer (k_{et}) on [M^{n+}] is derived from eq 4, as given by eq 6, where k_0 is the rate constant in the absence of M^{n+}.[29,30]

$$k_{et}/[M^{n+}] = k_0K_1(1 + K_2[M^{n+}]) \quad (6)$$

The validity of eq 6 is confirmed by the linear plot of k_{et} /[M^{n+}] versus [M^{n+}] for the Sc^{3+}- and Mg^{2+}-promoted electron transfer from CoTPP to Q, as shown in Figure 3a and b, respectively.[31] From the slopes and intercepts are obtained the K_2 value which is listed in Table 1 together with the k_0K_1 value.

There is a striking similarity with respect to the dependence of k_{et} (or k_{obs}) on [Sc^{3+}] and [Mg^{2+}] between the Sc^{3+}- and Mg^{2+}-promoted electron-transfer reactions from CoTPP to Q (Figure 1a and Figure 2a) and the Sc^{3+}- and Mg^{2+}-catalyzed Diels−Alder reaction of DMA with Q (Figure 1b and Figure 2b), respectively. Thus, the same plot as in eq 6 for the Sc^{3+}- and Mg^{2+}-promoted electron transfer from CoTPP to Q can be applied for the Sc^{3+}- and Mg^{2+}-catalyzed Diels−Alder reaction of DMA with Q, as shown in Figure 4a and b, respectively. The K_2 values for the 1:2 complex formation of $Q^{\bullet-}$ with Sc^{3+} and Mg^{2+} are obtained from the linear plots, as listed in Table 1. These K_2 values of Sc^{3+} ($4.0 \times 10\ M^{-1}$) and Mg^{2+} ($3.9\ M^{-1}$) derived from the metal ion-catalyzed Diels−Alder reaction of DMA with Q agree with those of Sc^{3+} ($4.0 \times 10\ M^{-1}$) and Mg^{2+} ($4.1\ M^{-1}$) derived from the metal ion-promoted electron transfer from CoTPP to Q in MeCN at 298 K.

(26) Mann, C. K.; Barnes, K. K. *Electrochemical Reactions in Nonaqueous Systems*; Marcel Dekker: New York, 1990.
(27) The direct determination measurements of the dependence of E_{red} on the M^{n+} concentration are difficult because of the instablity of the $Q^{\bullet-}$−M^{n+} complex. In the case of Mg^{2+}, the E_{red} values of Q in the presence of 0.1 M Mg^{2+} has been evaluated from the analysis of the one-electron reduction peak potential of Q as −0.18 V,[16b] from which the K_1 value is determined as $1.8 \times 10^6\ M^{-1}$ using eq 3 (the K_2 value is $4.1\ M^{-1}$, see Table 1).
(28) Fukuzumi, S.; Mochizuki, S.; Tanaka, T. *Inorg. Chem.* **1989**, *28*, 2459.
(29) The dependence of k_{et} on [M^{n+}] in eq 6 is derived on the basis of the Marcus theory of electron transfer which involves a strong interaction between an electron donor and acceptor (see Supporting Information, S3).[30]
(30) Marcus, R. A. *J. Phys. Chem.* **1968**, *72*, 891.
(31) Fukuzumi, S.; Ohkubo, K.; Tokuda, Y.; Suenobu, T. *J. Am. Chem. Soc.* **2000**, *122*, 4286.

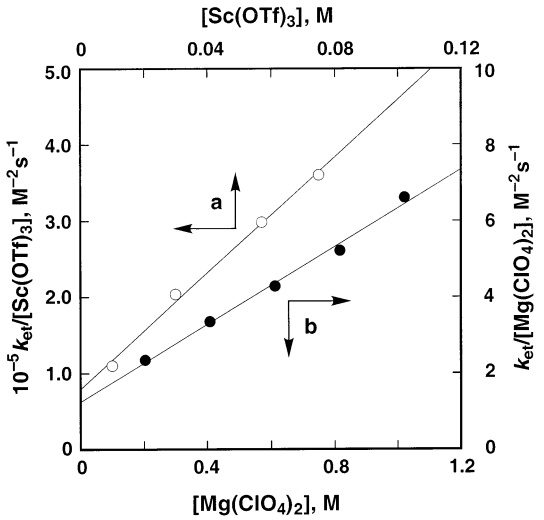

Figure 3. Plots of (a) $k_{obs}/[Sc(OTf)_3]$ vs $[Sc(OTf)_3]$ and (b) $k_{obs}/[Mg(ClO_4)_2]$ vs $[Mg(ClO_4)_2]$ for electron transfer from CoTPP to *p*-benzoquinone.

Since the metal ion acts as a Lewis acid in the complex formation with $Q^{\bullet-}$, the K_2 value is expected to increase or decrease, depending on the electron-donating or electron-withdrawing substituents X on Q. This was examined by determining the dependence of k_{obs} and k_{et} on $[M^{n+}]$ for the Sc^{3+}- and Mg^{2+}-catalyzed Diels−Alder reaction of DMA with X−Q and also the electron transfer from CoTPP to X−Q. The K_2 values determined by eq 6 are also listed in Table 1. The K_2 value (2.5×10 and $1.8\ M^{-1}$) determined in the Sc^{3+}- and Mg^{2+}-promoted electron transfer from CoTPP to a *p*-benzoquinone derivative with electron-withdrawing substituents (2,5-dichloro-*p*-benzoquinone) is smaller than the corresponding K_2 value of *p*-benzoquinone (4.0×10 and $4.1\ M^{-1}$), as expected from the weaker basicity of the radical anion with the electron-withdrawing substituents as compared to the basicity of unsubstituted semiquinone radical anion. In the case of *p*-fluoranil and *p*-chloranil, the K_2 values were too small to be determined because of the strong electron-withdrawing effects of fluorines and chlorines (Table 1). In contrast, the K_2 values of 2,5-dimethyl-*p*-benzoquinone, which has electron-donating substituents (4.3×10 and $4.7\ M^{-1}$ for Sc^{3+} and Mg^{2+}, respectively), are larger than those of *p*-benzoquinone. In each case, the K_2 value determined from the M^{n+}-catalyzed Diels−Alder reactions of DMA with X−Q agrees with the value determined from the corresponding M^{n+}-promoted electron-transfer reaction (Table 1). Such a remarkable agreement in each case strongly indicates that the M^{n+}-catalyzed Diels−Alder reactions of DMA with X−Q proceeds via the rate-determining M^{n+}-promoted electron transfer from DMA to X−Q, as shown in Scheme 1.

Such an M^{n+}-promoted electron-transfer pathway of X−Q has also been reported to occur in the M^{n+}-promoted hydride transfer from 10-methyl-9,10-dihydroacridine ($AcrH_2$) to X−Q (Scheme 2).[16a,27] In such a case, the same K_2 value should be derived from the dependence of k_{obs} on $[M^{n+}]$ for the M^{n+}-promoted hydride-transfer reactions from $AcrH_2$ to X−Q. This was also examined (see Supporting Information, S4), and the results are summarized in Table 1. The K_2 values determined from the M^{n+}-promoted hydride-transfer reactions from $AcrH_2$ to X−Q agree with those determined from the M^{n+}-catalyzed Diels−Alder reactions of DMA with X−Q as well as those determined from the corresponding M^{n+}-promoted electron-transfer reactions (Table 1). Such an agreement among three different systems confirms that each reaction has a common mechanism for the catalysis of metal ions, that is, the metal ion-promoted electron transfer.

When DMA is replaced by other anthracene derivatives, the reactivity decreases with increasing one-electron oxidation potentials (E°_{ox}) of anthracene derivatives. The k_0K_1 and K_2 values derived from the dependence of k_{obs} on $[Sc^{3+}]$ for the Sc^{3+}-catalyzed Diels−Alder reactions of anthracene derivatives with Q in MeCN at 333 K are listed in Table 2 together with the E°_{ox} values of anthracene derivatives. The K_2 values ($20-26\ M^{-1}$) are essentially the same within the experimental error, irrespective of the large difference in the reactivities of anthracene derivatives (see k_0K_1 values in Table 2). Such an agreement also confirms that the catalytic function of Sc^{3+} in the Diels−Alder reactions of anthracene derivatives with Q is ascribed to the formation of the 1:1 and 1:2 complex between $Q^{\bullet-}$ and Sc^{3+}, since the formation of the 1:2 complex of $Q^{\bullet-}$ and Mg^{2+} is independent of anthracene derivatives. The constant K_2 value ($1.9-2.6\ M^{-1}$), irrespective of the large difference in the reactivities of anthracene derivatives, is also confirmed for the Mg^{2+}-catalyzed Diels−Alder reactions of anthracene derivatives with Q in MeCN at 333 K (Table 2).[32]

The catalytic reactivity of metal ions varies significantly depending on the Lewis acidity of metal ions. The k_{cat} (k_0K_1) values of a series of metal ions for electron transfer from CoTPP to Q, the Diels−Alder reaction of DMA with Q, and the hydride-transfer reaction from $AcrH_2$ to Q were determined under the experimental conditions such that the k_{obs} value exhibits the first-order dependence with respect to the metal ion concentration. The results are summarized in Table 3.

We have recently reported that the binding energies (ΔE) of metal ions with $O_2^{\bullet-}$ can be evaluated from the deviation of the g_{zz} values from the free spin value and that the ΔE values are well correlated with the promoting effects of metal ions in the electron transfer from CoTPP to Q as well as O_2.[15] The ΔE values can, thereby, be used as the first quantitative measure for the Lewis acidity of metal ions in relation with the promoting effects of metal ions in electron-transfer reactions. Electron-transfer rates are expected to increase with decreasing E°_{ox} values of an electron donor and with increasing ΔE values. Figure 5a shows an excellent linear correlation between log k_{cat} and $E^\circ_{ox} - \Delta E$ for the M^{n+}-promoted electron transfer from CoTPP to Q.

Plots of log k_{cat} versus $E^\circ_{ox} - \Delta E$ for the M^{n+}-catalyzed Diels−Alder reactions of anthracene derivatives with Q (the data at 298 and 333 K are shown in Figure 5b and c, respectively) as well as the M^{n+}-promoted hydride transfer from $AcrH_2$ to Q (Figure 5d). There is a striking parallel relationship between the M^{n+}-promoted electron transfer and the M^{n+}-catalyzed Diels−Alder reactions as well as the M^{n+}-promoted hydride-transfer reactions. The catalytic reactivities of different metal ions in each reaction are well correlated with the ΔE values. The difference in the reactivities of anthracene derivatives and $AcrH_2$ is also well correlated with the E°_{ox} values in the linear plot of log k_{cat} versus $E^\circ_{ox} - \Delta E$. This indicates that the activation process is common between the Diels−Alder

(32) The K_2 value at 333 K (Table 2) is smaller than the corresponding value at 298 K (Table 1) because of the negative value of enthalpy of the complex formation.

Table 1. Rate Constants of Electron Transfer, Diels−Alder, and Hydride Transfer Reactions in the Absence Sc^{3+} (k_0) and in the Presence of Sc^{3+} and Mg^{2+} (k_0K_1) and the Formation Constants of X−$Q^{\bullet-}$−$2Sc^{3+}$ and X−$Q^{\bullet-}$−$2Mg^{2+}$ (K_2) in Deaerated MeCN at 298 K

		CoTPP		DMA		$AcrH_2$	
X–Q	metal ion	k_0K_1[a] (M^{-2} s^{-1})	K_2[a] (M^{-1})	k_0K_1[a] (M^{-2} s^{-1})	K_2[a] (M^{-1})	k_0K_1[a] (M^{-2} s^{-1})	K_2[a] (M^{-1})
Q	Sc^{3+}	2.7×10^5	4.0×10	1.3	4.0×10	7.2×10^4	3.9×10
Q	Mg^{2+}	1.3×10	4.1	6.9×10^{-3}	3.9	2.0	4.0
2,5-Cl_2Q	Sc^{3+}	9.3×10^5	2.5×10	1.1×10	2.1×10	2.4×10^5	2.3×10
2,5-Cl_2Q	Mg^{2+}	1.2	1.8	4.9×10^{-3}	1.6	8.2	1.6
2,5-Me_2Q	Sc^{3+}	1.1×10^5	4.3×10	1.2×10	4.4×10	3.0×10^4	4.3×10
2,5-Me_2Q	Mg^{2+}	8.9×10^{-1}	4.7	1.3×10^{-3}	4.6	1.0×10^{-1}	4.0
F_4Q	Sc^{3+}	1.1×10^6	0	4.9×10^{-2}	0	3.0×10^4	0
F_4Q	Mg^{2+}	2.8×10^2	0	5.7×10^{-4}	0	4.0×10	0
Cl_4Q	Sc^{3+}	1.0×10^6	0	*b*	*b*	2.9×10^4	0
Cl_4Q	Mg^{2+}	2.2×10^2	0	*b*	*b*	5.3×10	0

[a] Determined from the dependence of k_{et} or k_{obs} on the concentration of metal ion based on eq 6. [b] No reaction.

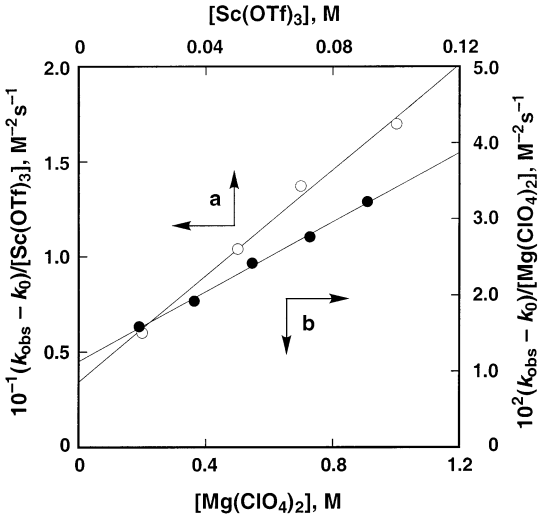

Figure 4. Plots of (a) $(k_{obs} - k_0)/[Sc(OTf)_3]$ vs $[Sc(OTf)_3]$ and (b) $(k_{obs} - k_0)/[Mg(ClO_4)_2]$ vs $[Mg(ClO_4)_2]$ for the Diels−Alder reaction of 9,10-dimethylanthracene with *p*-benzoquinone.

Scheme 1

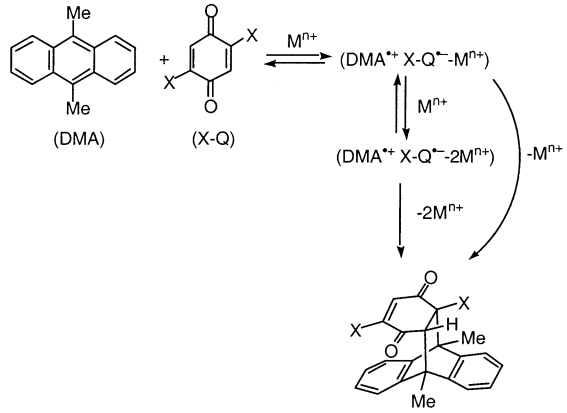

reaction (Scheme 1) and the hydride-transfer reaction (Scheme 2), that is, the metal ion-promoted electron transfer.

The rates of M^{n+}-catalyzed hydride-transfer reactions from $AcrH_2$ ($E°_{ox}$ vs SCE = 0.81 V)[16a] to Q (Figure 5d) are slightly faster than those of the Diels−Alder reactions of DMA ($E°_{ox}$ = 1.05 V) with Q (Figure 5b) when they are compared at the same $E°_{ox} - \Delta E$ values.[33] This indicates that the proton transfer from $AcrH_2^{\bullet+}$ to the $Q^{\bullet-}$−M^{n+} complex after the M^{n+}-promoted

(33) The k_{cat} values in Figure 5c are larger than those in Figure 5b because of the higher reaction temperature (333 K in Figure 5c as compared to 298 K in Figure 5b).

Scheme 2

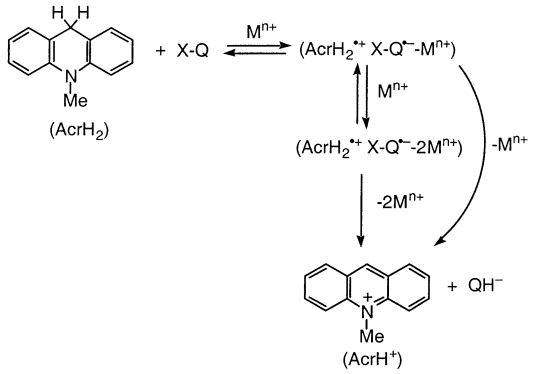

Table 2. Rate Constants of Diels−Alder Reactions of Anthracene Derivatives with *p*-Benzoquinone in the Absence of Metal Ion (k_0) and in the Presence of Metal Ion (k_0K_1) and the Formation Constants of the 1:2 Complexes of the Corresponding Radical Anions with Metal Ion (K_2) in Deaerated MeCN at 333 K

no.	donor	E^0_{ox} V vs SCE	metal ion	k_0K_1[a] (M^{-2} s^{-1})	K_2[a] (M^{-1})
1	9,10-dimethylanthracene	1.05	Sc^{3+}	8.3	2.0×10
2	9-methylanthracene	1.11	Sc^{3+}	2.1	2.2×10
3	9-ethylanthracene	1.14	Sc^{3+}	3.4×10^{-1}	2.6×10
4	anthracene	1.19	Sc^{3+}	7.1×10^{-2}	2.0×10
5	9-benzylanthracene	1.20	Sc^{3+}	3.2×10^{-1}	2.0×10
6	9-bromoanthracene	1.30	Sc^{3+}	3.3×10^{-3}	2.1×10
7	9,10-dimethylanthracene	1.05	Mg^{2+}	3.5×10^{-2}	2.5
8	9-methylanthracene	1.11	Mg^{2+}	6.2×10^{-3}	1.9
9	9-ethylanthracene	1.14	Mg^{2+}	4.3×10^{-4}	2.6
10	anthracene	1.19	Mg^{2+}	1.4×10^{-4}	2.0

[a] Determined from the dependence of k_{obs} on $[Sc^{3+}]$ based on eq 6.

electron transfer in Scheme 1 is slightly faster than the C−C bond formation in the radical ion pair ($DMA^{\bullet+}Q^{\bullet-}$−$M^{n+}$) in Scheme 2. Such a difference is much enhanced when Q is replaced by *p*-chloranil (Cl_4Q) because of the steric effects of chlorines. Since the steric effect is more pronounced in the C−C bond formation than in the proton transfer, no Diels−Alder reaction occurs between DMA and Cl_4Q, whereas the hydride transfer from $AcrH_2$ to Cl_4Q occurs efficiently (see Table 1).

Detection of Metal Ion Complexes with Semiquinone Radical Anions. When CoTPP is replaced by a stronger one-electron reductant, decamethylferrocene [$Fe(C_5Me_5)_2$], electron transfer from $Fe(C_5Me_5)_2$ to Q in the presence of $Mg(ClO_4)_2$ is complete upon mixing the two solutions. The transient electronic spectra of the semiquinone radical anion in the presence of different concentrations of $Mg(ClO_4)_2$ were obtained by measuring the change in initial absorbance at various wavelengths with

Table 3. Catalytic Rate Constants ($k_{cat} = k_0K_1$) for the Electron Transfer from CoTPP to *p*-Benzoquinone, Diels−Alder Reaction of DMA with *p*-Benzoquinone, and Hydride Transfer from $AcrH_2$ to *p*-Benzoquinone in Deaerated MeCN at 298 K

		k_{cat} (M^{-2} s^{-1})		
M^{n+}	ΔE^a (eV)	CoTPP[a]	DMA	$AcrH_2$
Sc^{3+}	1.00	2.7×10^5	1.3	7.2×10^4
Y^{3+}	0.85	2.7×10^3	3.7×10^{-2}	2.1×10^3
La^{3+}	0.82	1.9×10^3	1.4×10^{-2}	
Eu^{3+}	0.82	1.1×10^3	1.9×10^{-2}	
Yb^{3+}	0.83	1.2×10^3	4.5×10^{-2}	
Lu^{3+}	0.83	8.2×10^2	4.1×10^{-2}	1.8×10^3
Mg^{2+}	0.65	1.3	6.9×10^{-3}	2.0
Ca^{2+}	0.58	7.0×10^{-1}		2.9×10^{-1}
Sr^{2+}	0.52	1.6×10^{-1}		
Ba^{2+}	0.49	3.0×10^{-2}		
Li^+	0.53	1.6×10^{-1}		

[a] Taken from ref 15.

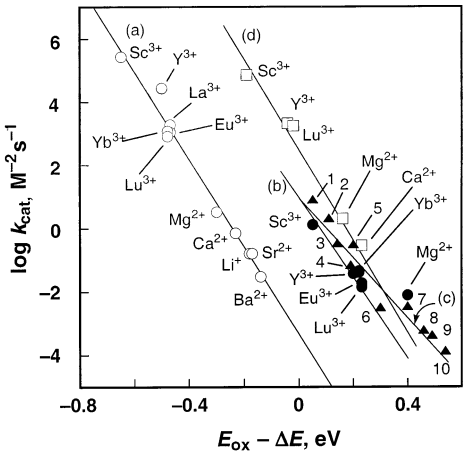

Figure 5. Plots of log k_{cat} vs ($\Delta E_{ox} - \Delta E$) for the (a) electron-transfer reaction from CoTPP to *p*-benzoquinone at 298 K (○), (b) Diels−Alder reaction of 9,10-dimethylanthracene with *p*-benzoquinone at 298 K (●), (c) Diels−Alder reaction of anthracene derivatives with *p*-benzoquinone at 333 K (▲), and (d) hydride-transfer reaction from $AcrH_2$ to *p*-benzoquinone at 298 K (□), in the presence of metal ions in deaerated MeCN. Numbers refer to anthracence derivatives in Table 2.

the use of a stopped-flow spectrophotometer, as shown in Figure 6.[34] The absorption spectrum of $Q^{\bullet-}$ in the presence of 1.0×10^{-2} M Mg^{2+} ($\lambda_{max} = 590$ nm) is significantly red-shifted as compared to that in the absence of Mg^{2+} ($\lambda_{max} = 422$ nm). The further addition of Mg^{2+} results in a blue shift to $\lambda_{max} = 415$ nm with a clean isosbestic point. Such spectroscopic changes indicate the formation of complexes between $Q^{\bullet-}$ and Mg^{2+}, which requires two steps: the first step is the formation of a 1:1 complex ($Q^{\bullet-}$-Mg^{2+}), and the second step is an additional addition of Mg^{2+} to form a 1:2 complex ($Q^{\bullet-}-2Mg^{2+}$). Transient electronic spectra of the 1:1 and 1:2 complexes are also observed in the electron-transfer reduction of 2,5-dichloro-*p*-benzoquinone (Figure 7) and 2,5-dimethyl-*p*-benzoquinone. Although the formation constant K_1 for the 1:1 complex is too large to be determined, the formation constant K_2 for the 1:2 complex can be determined from the spectral change in the presence of Mg^{2+} using eq 7,

$$A^{-1} = A_0^{-1}(1 + K_2[Mg(ClO_4)_2]) \quad (7)$$

(34) For the absorption spectrum of $Q^{\bullet-}$ in the absence of Mg^{2+} in MeCN, see: Fukuzumi, S.; Yorisue, T. *J. Am. Chem. Soc.* **1991**, *113*, 7764.

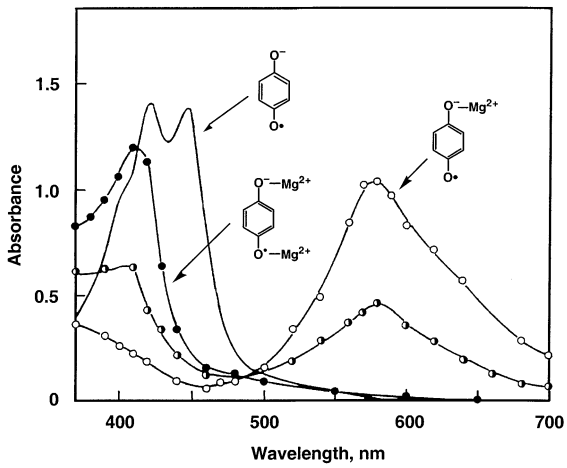

Figure 6. Transient absorption spectra of the semiquinone radical anion formed in the electron-transfer reduction of *p*-benzoquinone (2.4×10^{-3} M) by [$Fe(Me_5C_5)_2$] (2.4×10^{-4} M) in the presence of $Mg(ClO_4)_2$ [1.0×10^{-2} M (○), 2.0×10^{-1} M (◑)] and by [$Fe(MeC_5H_4)_2$] (2.4×10^{-4} M) in the presence of $Mg(ClO_4)_2$ [1.6 M (●)] in deaerated MeCN at 298 K. The solid line spectrum shows the absorption spectrum of the semiquinone radical anion in the absence of $Mg(ClO_4)_2$, prepared by the reaction of *p*-benzoquinone (2.4×10^{-3} M) with $Me_4N^+OH^-$ (2.4×10^{-4} M) in deaerated MeCN at 298 K.

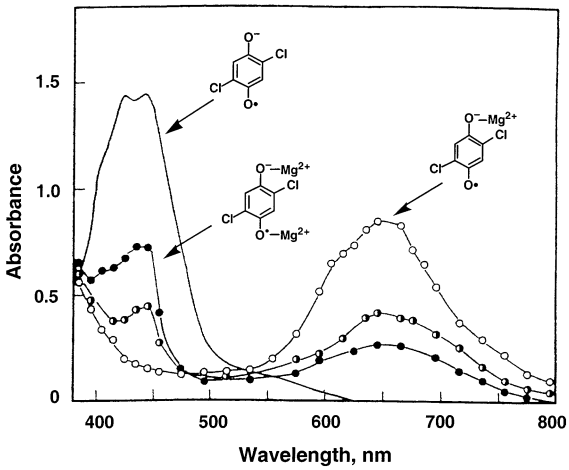

Figure 7. Transient absorption spectra of the semiquinone radical anion formed in the electron-transfer reduction of 2,5-dichloro-*p*-benzoquinone (2.4×10^{-3} M) by [$Fe(Me_5C_5)_2$] (2.4×10^{-4} M) in the presence of $Mg(ClO_4)_2$ [5.0×10^{-3} M (○), 4.0×10^{-1} M (◑)] and by [$Fe(MeC_5H_4)_2$] (2.4×10^{-4} M) in the presence of $Mg(ClO_4)_2$ [1.0 M (●)] in deaerated MeCN at 298 K. The solid line spectrum shows the absorption spectrum of the semiquinone radical anion in the absence of $Mg(ClO_4)_2$, prepared by the reaction of 2,5-dichloro-*p*-benzoquinone (2.4×10^{-4} M) with $Me_4N^+OH^-$ (2.4×10^{-4} M) in deaerated MeCN at 298 K.

where *A* is the absorbance due to the 1:1 complex and A_0 is the initial absorbance at the small concentration of Mg^{2+}. From the linear plots of A^{-1} versus [$Mg(ClO_4)_2$] (see Supporting Information S5), the K_2 values for the 1:2 complexes formed between $X-Q^{\bullet-}$ and Mg^{2+} are obtained, as listed in Table 4, together with the absorption maxima of $X-Q^{\bullet-}$ and the 1:1 and 1:2 complexes with Mg^{2+}. The K_2 values thus determined directly from the spectral change due to the complex formation between $X-Q^{\bullet-}$ and Mg^{2+} (Table 4) agree with those determined from the dependence of k_{obs} on [Mg^{2+}] for the Mg^{2+}-promoted electron transfer from CoTPP to X−Q, the Mg^{2+}-catalyzed Diels−Alder reaction of DMA with Q, and the Mg^{2+}-catalyzed hydride transfer from $AcrH_2$ to Q (Table 1). Thus, the catalysis of Mg^{2+} in the electron-transfer reduction of *p*-benzoquinone

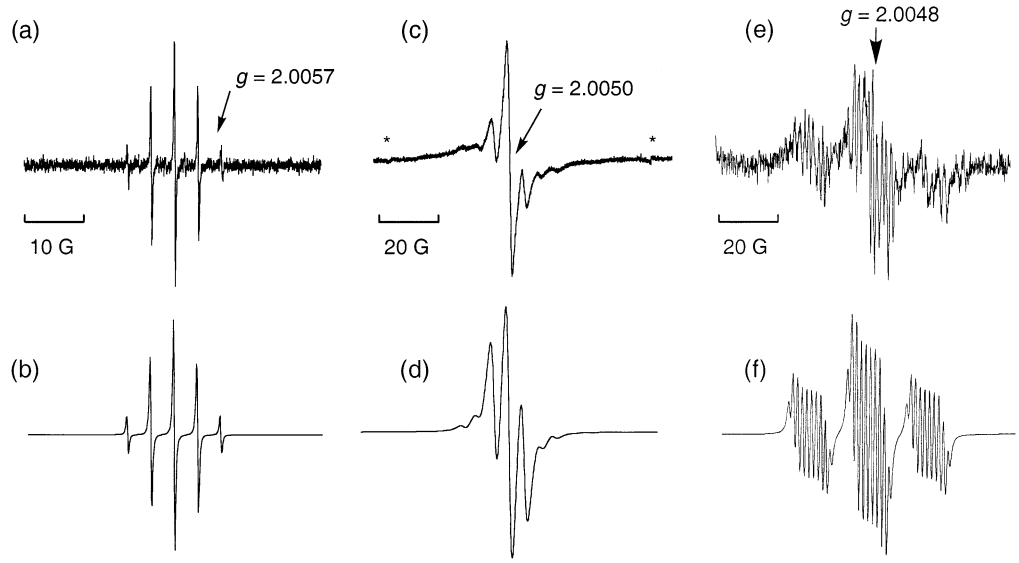

Figure 8. (a) ESR spectrum of the *p*-fluoranil radical anion formed in the electron-transfer reduction of *p*-fluoranil (2.0×10^{-5} M) by $(BNA)_2$ (1.0×10^{-5} M) in deaerated MeCN at 298 K. (b) Computer simulation spectrum with $g = 2.0057$ with $a(4\text{ F}) = 3.9$ G and $\Delta H_{msl} = 0.20$ G. (c) ESR spectrum of the *p*-fluoranil radical anion−$Mg(ClO_4)_2$ complex generated in the photoirradiation of a deaerated MeCN solution of *p*-fluoranil (1.0×10^{-3} M) with $(BNA)_2$ (1.0×10^{-3} M) in the presence of $Mg(ClO_4)_2$ (1.0 M) at 298 K. Asterisks denote Mn^{2+} markers. (d) Computer simulation spectrum with $g = 2.0050$ with $a(2\text{ F}) = 5.0$ G, $a(^{25}\text{Mg}) = 4.1$ G, and $\Delta H_{msl} = 2.0$ G. (e) ESR spectrum of the *p*-fluoranil radical anion−$Sc(OTf)_3$ complex generated in the photoirradiation of a deaerated MeCN solution of fluoranil (5.0×10^{-3} M) with $(BNA)_2$ (1.0×10^{-3} M) in the presence of $Sc(OTf)_3$ (1.0×10^{-3} M) at 243 K. (f) Computer simulation spectrum with $g = 2.0048$ with $a(2\text{F}) = 10.0$ G, 0.7 G, $a(\text{Sc}) = 0.8$ G, and $\Delta H_{msl} = 0.4$ G.

Table 4. Absorption Maxima (λ_{max}) of Semiquinone Radical Anions ($X-Q^{\bullet-}$) and the $X-Q^{\bullet-}-Mg^{2+}$ and $X-Q^{\bullet-}-2Mg^{2+}$ Complexes Formed by the Electron Transfer Reduction of *p*-Benzoquinone and Its Derivatives in the Presence of $Mg(ClO_4)_2$ and the Formation Constants of $Q^{\bullet-}-2Mg^{2+}$ (K_2) in Deaerated MeCN at 298 K

	λ_{max} (nm)			
X–Q	$X-Q^{\bullet-}$	$X-Q^{\bullet-}-Mg^{2+}$	$X-Q^{\bullet-}-2Mg^{2+}$	K_2[a]
Q	422	590	410	4.5
2,5-C_{12}Q	425	645	440	2.1
2,5-Me_2Q	436	615	425	4.8

[a] Determined from the spectral change in the presence of Mg^{2+}.

derivatives is indeed ascribed to the formation of 1:1 and 1:2 complexes formed between $X-Q^{\bullet-}$ and Mg^{2+}, which results in an increase in the rate constants of electron transfer from CoTPP to X−Q, the Diels−Alder reactions of anthracenes with X−Q, and hydride-transfer reactions from $AcrH_2$ to X−Q with an increase in $[Mg^{2+}]$, exhibiting first-order and second-order dependence on $[Mg^{2+}]$.

The K_2 value decreases with the decreasing electron-donor ability of $X-Q^{\bullet-}$ (X = 2,5-Me_2 > H > 2,5-Cl_2). In the case of *p*-fluoranil (F_4Q), only the 1:1 complex is formed between $F_4Q^{\bullet-}$ and Mg^{2+} because of the strong electron-withdrawing effect of fluorines. The formation of the 1:1 $F_4Q^{\bullet-}-Mg^{2+}$ complex is confirmed by the ESR spectrum. First, $F_4Q^{\bullet-}$ is formed by electron transfer from dimeric 1-benzyl-1,4-dihydronicotinamide $[(BNA)_2]$[22b] to Q in MeCN at 298 K. The $(BNA)_2$ is known to act as a unique electron donor to produce the radical anions of electron acceptors.[35] The ESR spectrum of $F_4Q^{\bullet-}$ is shown in Figure 8a, together with the computer simulation spectrum with the hyperfine coupling constant [hfc; $a(4\text{F}) = 3.9$ G] (Figure 8b).[36] Wheeler et al.[37] calculated the hfc values of semiquinone anion radicals using various density functional (DF) and hybrid Hartree−Fock/density functional (HF/DF) methods. The best method to predict the hfc value of $Q^{\bullet-}$, however, affords a much smaller hfc value ($a(4\text{F}) = 1.95$ G)[37] than the experimental value ($a(4\text{F}) = 3.9$ G).

The addition of $Mg(ClO_4)_2$ (1.0 M) to an MeCN solution of $F_4Q^{\bullet-}$ affords the ESR spectrum in Figure 8c. The observed ESR spectrum is well reproduced by the computer simulation spectrum with the hfc values including a superhyperfine coupling due to one ^{25}Mg nucleus ($a(\text{Mg}) = 4.1$ G) which has 10.13% natural abundance, as shown in Figure 8d. The observation of such a superhyperfine coupling due to one magnesium nucleus strongly indicates the formation of the 1:1 complex between $F_4Q^{\bullet-}$ and Mg^{2+}.[38,39] Because of the complexation with one Mg^{2+}, the spin is more localized on two carbons, as shown in Scheme 3. The hyperconjugation to the fluorine atom (Scheme 3) of the $F_4Q^{\bullet-}-Mg^{2+}$ complex results in an increase in the $a(2\text{F})$ value (5.0 G) as compared to the value of $F_4Q^{\bullet-}$ (3.9 G).[40]

The 1:1 complex between $F_4Q^{\bullet-}$ and Sc^{3+} is also formed as the case of $F_4Q^{\bullet-}-Mg^{2+}$ complex (Figure 8c), and the ESR spectrum is shown in Figure 8e. The computer simulation spectrum in Figure 8f affords the hfc values, including a superhyperfine coupling due to one scandium nucleus (a(Sc)

(35) Fukuzumi, S.; Suenobu, T.; Patz, M.; Hirasaka, T.; Itoh, S.; Fujitsuka, M.; Ito, O. *J. Am. Chem. Soc.* **1998**, *120*, 8060.

(36) A slightly larger a(4F) value (4.14 G) was reported for $F_4Q^{\bullet-}$ in ethanolic KOH solution. See: Anderson, D. H.; Frank, P. J.; Cutowsky, H. S. *J. Chem. Phys.* **1960**, *32*, 196.

(37) Boesch, S. E.; Wheeler, R. A. *J. Phys. Chem. A* **1997**, *101*, 8351.

(38) Although X-ray diffraction structures are available for crystals containing *p*-chloranil radical anion−alkai metal ion complexes,[39] analogous structures for the *p*-fluoranil radical anion−metal ion complex are unavailable.

(39) Konno, M.; Kobayashi, H.; Marumo, F.; Saito, Y. *Bull. Chem. Soc. Jpn.* **1973**, *46*, 1987.

(40) The spin density on the fluorine atom is determined mainly by the direct spin delocalization due to the hyperconjugation which induces a positive spin density in contrast with the spin polarization which induces a negative spin density.

Scheme 3

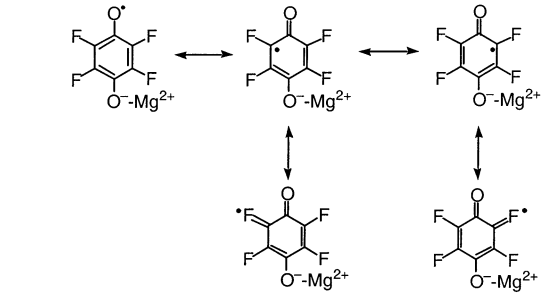

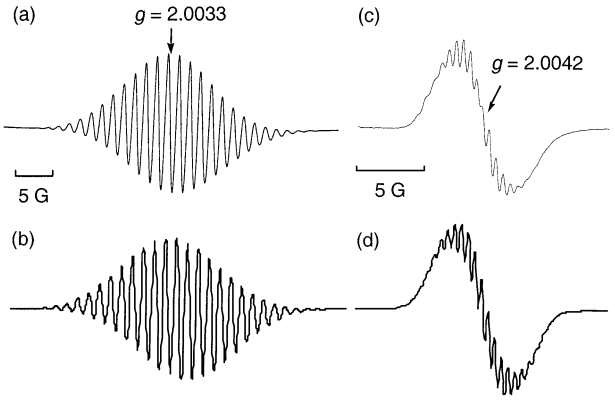

Figure 9. (a) ESR spectrum of propionitrile solution containing $(BNA)_2$ (3.4×10^{-3} M), 2,5-dimethyl-*p*-benzoquinone (1.1×10^{-2} M), and $Sc(OTf)_3$ (3.4×10^{-3} M), irradiated with a high-pressure mercury lamp at 203 K. (b) Computer simulation spectrum with $g = 2.0033$ with $a(6\text{ H}) = 2.8$ G, $a(2\text{H}) = 1.8$ G, $a(2\text{Sc}) = 1.5$ G, and $\Delta H_{msl} = 0.40$ G. (c) ESR spectrum of propionitrile solution containing $(BNA)_2$ (3.5×10^{-3} M), 2,5-dichloro-*p*-benzoquinone (9.7×10^{-3} M), and $Sc(OTf)_3$ (2.5×10^{-1} M), irradiated with a high-pressure mercury lamp at 203 K. (d) Computer simulation spectrum with $g = 2.0043$ with $a(^{35}\text{Cl}) = 0.5$ G, $a(2\text{ H}) = 0.2$ G, $a(2\text{ Sc}) = 0.5$ G, and $\Delta H_{msl} = 0.30$ G.

$= 0.8$ G).[41] This is consistent with the first-order dependence of k_{obs} on $[Sc^{3+}]$ for the Sc^{3+}-promoted electron transfer from CoTPP to F_4Q, the Diels–Alder reaction of DMA with F_4Q, and the hydride transfer from $AcrH_2$ to F_4Q.

The 1:2 complex formation between $Q^{\bullet-}$ and Sc^{3+} has also been confirmed by observation of the ESR spectrum of the $Q^{\bullet-}$–$2Sc^{3+}$ complex which shows the superhyperfine structure due to the interaction of $Q^{\bullet-}$ with two equivalent Sc nuclei, as reported previously.[17] Since the $Q^{\bullet-}$–$2Sc^{3+}$ complex is unstable because of the facile disproportionation reaction, the complex was generated in photoinduced electron transfer from dimeric 1-benzyl-1,4-dihydronicotinamide [$(BNA)_2$] to Q at low temperatures. Propionitrile was used instead of MeCN to avoid freezing the solvent at 203 K. Similarly, the 1:2 complex formation between the radical anion of 2,5-dimethyl-*p*-benzoquinone ($2,5\text{-}Me_2Q^{\bullet-}$) and Sc^{3+} is confirmed by the ESR spectra of the $2,5\text{-}Me_2Q^{\bullet-}$–$2Sc^{3+}$ complex and the corresponding computer simulation spectra, as shown in Figure 9a and b, respectively. The superhyperfine structure due to two equivalent Sc nuclei [$a(2\text{Sc}) = 1.5$ G] confirms the formation of the 1:2 complex between $2,5\text{-}Me_2Q^{\bullet-}$ and Sc^{3+}. The ESR spectrum of the radical anion of 2,5-dichloro-*p*-benzoquinone ($2,5\text{-}Cl_2Q^{\bullet-}$) in the presence of $Sc(OTf)_3$ (2.5×10^{-1} M) (Figure 9c) also exhibits the superhyperfine structure due to two equivalent Sc nuclei, as shown in the computer simulation spectrum (Figure 9d). The smaller $a(2\text{Sc})$ value of the $2,5\text{-}Cl_2Q^{\bullet-}$–$2Sc^{3+}$ complex (0.5 G) compared with the value of the $2,5\text{-}Me_2Q^{\bullet-}$–$2Sc^{3+}$ complex (1.5 G) is consistent with the smaller K_2 value of the former compared with that of the latter (Table 1).

(41) The stronger the binding between $F_4Q^{\bullet-}$ and the metal ion, the larger the $a(2\text{F})$ value (10 G) for the Sc^{3+} complex as compared with 5.0 G for the Mg^{2+} complex (Scheme 3).

Summary and Conclusions

Extensive comparisons of the metal ion catalysis among the M^{n+}-promoted electron transfer, hydride transfer, and Diels–Alder reactions of *p*-benzoquinone derivatives have revealed that the origin of the metal ion catalysis is all in common. Namely, the formation of 1:1 and 1:2 complexes formed between $X\text{–}Q^{\bullet-}$ and M^{n+} results in an increase in not only the rates of electron transfer from CoTPP but also in the rates of Diels–Alder reactions of anthracenes with X–Q as well as the hydride-transfer reactions from $AcrH_2$ to X–Q, in which the rate-determining step is M^{n+}-promoted electron transfer, exhibiting first-order and second-order dependence on $[M^{n+}]$, respectively. The formation of 1:1 and 1:2 complexes formed between $X\text{–}Q^{\bullet-}$ and M^{n+} has been confirmed by the direct spectroscopic detection of the transient absorption spectra and the ESR spectra. The catalytic reactivities of a variety of metal ions are well correlated with the Lewis acidities of metal ions, derived quantitatively as the energy splitting values of π_g levels due to the complex formation between $O_2^{\bullet-}$ and M^{n+} from the g_{zz} values of the ESR spectra.

Acknowledgment. This work was partially supported by a Grant-in-Aid for Scientific Research Priority Area (No. 11228205) from the Ministry of Education, Science, Culture and Sports, Japan.

Supporting Information Available: Kinetic data for the Sc^{3+}-catalyzed Diels–Alder reaction (S1), ^{13}C chemical shifts of *p*-benzoquinone in the presence of Mg^{2+} (S2), derivation of eq 6 (S3), kinetic data for the Sc^{3+}- and Mg^{2+}-promoted hydride-transfer reactions from $AcrH_2$ to Q (S4), and plot of A^{-1} of the $X\text{–}Q^{\bullet-}$-Mg^{2+} complex versus $[Mg^{2+}]$ (S5). This material is available free of charge via the Internet at http://pubs.acs.org.

JA026417H